Robotica (2005) volume 23, pp. 377–386. © 2005 Cambridge University Press
doi:10.1017/S0263574704000992 Printed in the United Kingdom

On stiffness improvement of the Tricept machine tool

Dan Zhang

Faculty of Engineering and Applied Science, University of Ontario Institute of Technology, Oshawa, Ontario (Canada) L1H 7K4 E-mail: Dan.Zhang@uoit.ca

(Received in Final Form: July 29, 2004)

SUMMARY

In this paper, an alternate passive leg structure is proposed for the Tricept machine tool to form a modified Tricept machine tool. The global stiffness of the modified Tricept machine tool is derived and compared with that of the Tricept machine tool. First, the configurations of the Tricept machine tool and the modified Tricept machine tool are introduced, respectively. Then, the global velocity equations are derived and the stiffness models of the two configurations are presented and analyzed. Finally, the advantages and disadvantages of the two types of passive leg structure are analyzed and discussed and stiffness simulations are conducted.

KEYWORDS: Triceps machine tool; Stiffness improvement; Passive leg structure

1. INTRODUCTION

Parallel Kinematic Machines (PKM) are machines based on parallel mechanisms. As parallel mechanism has the potential advantages of high stiffness, high speed, high dexterity, low inertia and large payload capacity, research in parallel mechanisms has been growing since the 1960s. The first Hexapod machine was designed by Gough[1] as a tire testing machine and then by Stewart[2] for use in an aircraft simulator. Over the past decades, parallel mechanisms have received more and more attention from researchers and industries. They can be found in several practical applications, such as aircraft simulators,[3] adjustable articulated trusses,[4] mining machines,[5] pointing devices[6] and micro-positioning devices.[7] More recently, they have been developed as high precision machine tools[8–12] by many companies such as Giddings & Lewis, Ingersoll, SMT Tricept, Geodetic and Toyoda, etc. Among them the Tricept machine tools[13,14] are one of the successful applications.

Since most machining operations only require a maximum of 5 axes (degrees of freedom), new configurations with less than six axes (degrees of freedom) would be more appropriate. Tripod is one type of a parallel kinematic machine with three degrees of freedom, and it can realize the three axes machining, therefore, the Tripod is targeted as the main configuration for PKMs development. Examples include ABB Delta robot, Tricept,[15] Gerog V,[16] Triaglide[17] and Z^3 head.[18] Tripod can be combined with two axis systems, such as x-y table, to form five axis machines.

In this paper, an alternate passive link structure for Tricept is proposed. The configurations of the Tricepts with different passive links are described first. Then the kinematics, including the Jacobian matrix and velocity equation, are derived, and the stiffness models for the two types of Tricept with rigid links and with flexible links are presented and discussed. Finally, the comparison of the two configurations of Tricept with/without the consideration of flexible links is conducted and conclusions are given.

2. GEOMETRIC MODELING

2.1. Tricept machine tool

As shown in Figure 1, the Tricept machine tools family are developed by SMT Tricept. It is designed as a vertical machining center. The range of application includes HSC-milling of aluminum, steel, structural parts, composites and riveting for the aerospace as well as large model making, plastic and foam machining for automation, all types of laser cutting, water jet and welding applications.

The schematic representation of the Tricept machine tool and the geometry of the joint distribution both on the base and platform are shown in Figures 2 and 3. This mechanism consists of four kinematic chains, including three variable length legs with identical topology and one passive leg, connecting the fixed base to the moving platform. In this 3-dof parallel mechanism, the kinematic chains associated with the three identical legs consist, from base to platform, of a fixed U-joint, a moving link, an actuated prismatic joint, a moving link and a spherical joint attached to the platform. The fourth chain connecting the base center to the platform is a passive leg and has an architecture different from the other three identical chains. It consists of a fixed U-joint, a prismatic joint attached to the base, a moving link fixed to the platform. This last leg is used to constrain the motion of the platform to only three degrees of freedom.

2.2. The modified Tricept machine tool

As represented in Figure 4, the modified Tricept machine tool has 3DOF, it also consists of four kinematic chains, including three variable length legs with identical topology as Tricept and one passive leg which is different from that of Tricept, connecting the fixed base to a moving platform. The fourth chain connecting the base center to the platform center is a passive constraining leg and has a different architecture from the other three identical chains. It consists of a prismatic joint

Fig. 1. Tricept machine tools prototype.

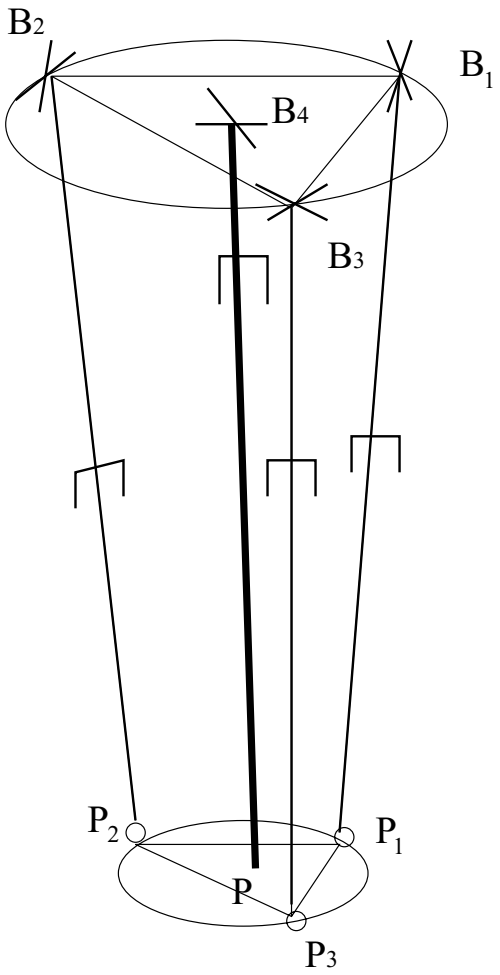

Fig. 2. Schematic representation of the Tricept machine tool.

attached to the base, a moving link and a U-joint attached to the platform. The positions of the attachment points on the base and platform are the same as Figure 3.

3. KINEMATIC MODELING FOR THE ACTUATED PART

As the two mechanisms have the identical actuated parts, they have the same kinematic equations as well. Since the platform of the two mechanisms has three degrees of freedom, only three of the six Cartesian coordinates of the platform are independent. For the Tricept mechanism of Figure 2, the independent coordinates have been chosen for convenience as $(z, \theta_{41}, \theta_{42})$, where $(\theta_{41}, \theta_{42})$ are the joint angles of the U-joint attached to the base center. For the modified Tricept one, the independent coordinates have been chosen as $(z, \theta_{m42}, \theta_{m43})$, where θ_{m42}, θ_{m43} are the joint angles of the U-joint attached to the platform.

Assume that the vertices located on the base and the platform are located on circles with radii R_b and R_p, respectively. A fixed reference frame $O - xyz$ is attached to the base of the mechanism and a moving coordinate frame $P - x'y'z'$ is attached to the platform. In the figure, the points of attachment of the actuated legs to the base are represented with B_i and the points of attachment of all legs to the platform are represented with P_i, with $i = 1, \ldots, 4$. Point P is located

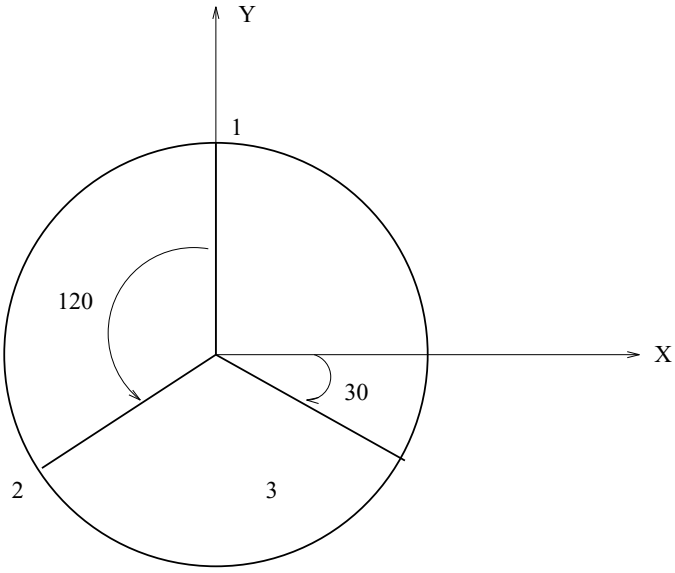

Fig. 3. Position of the attachment points on the base and platform.

at the center of the platform and its position coordinates are $P(x, y, z)$ $(P(4) = P)$.

The Cartesian coordinates of the platform are given by the position of point P with respect to the fixed frame, and the orientation of the platform (orientation of frame $P - x'y'z'$ with respect to the fixed frame), represented by matrix $\mathbf{Q}$.

https://doi.org/10.1017/S0263574704000992 Published online by Cambridge University Press

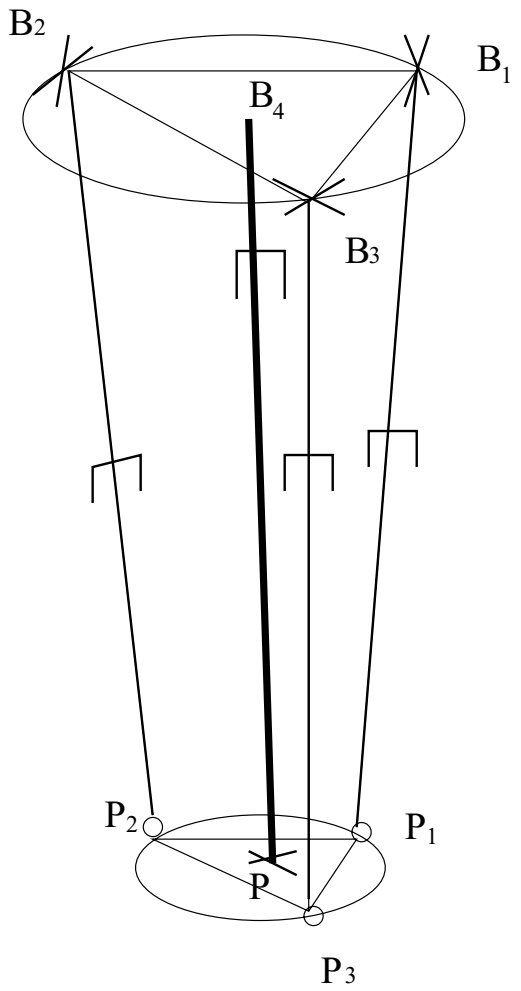

Fig. 4. Schematic representation of the modified Tricept machine tool.

If the coordinates of the point P_i in the moving reference frame are represented with (x_i', y_i', z_i') and the coordinates of the point B_i in the fixed frame are represented by vector $\mathbf{b}_i$, then for $i = 1, \ldots, 4$, one has

$$\mathbf{p}_i = \begin{bmatrix} x_i \\ y_i \\ z_i \end{bmatrix} \quad \mathbf{r}_i' = \begin{bmatrix} x_i' \\ y_i' \\ z_i' \end{bmatrix} = \begin{bmatrix} 0 \\ -R_p \sin\theta_{pi} \\ R_p \cos\theta_{pi} \end{bmatrix}$$
$$\mathbf{p} = \begin{bmatrix} x \\ y \\ z \end{bmatrix} \quad \mathbf{b}_i = \begin{bmatrix} b_{ix} \\ b_{iy} \\ b_{iz} \end{bmatrix} = \begin{bmatrix} R_b \cos\theta_{bi} \\ R_b \sin\theta_{bi} \\ 0 \end{bmatrix} \tag{1}$$

where $\mathbf{p}_i$ is the position vector of point P_i expressed in the fixed coordinate frame whose coordinates are defined as (x_i, y_i, z_i), $\mathbf{r}_i'$ is the position vector of point P_i expressed in the moving coordinate frame, and $\mathbf{p}$ is the position vector of point P expressed in the fixed frame as defined above, and

$$\boldsymbol{\theta}_{bi} = \begin{bmatrix} \theta_{b1} \\ \theta_{b2} \\ \theta_{b3} \end{bmatrix} = \begin{bmatrix} \pi/2 \\ 7\pi/6 \\ -\pi/6 \end{bmatrix} \quad \boldsymbol{\theta}_{pi} = \begin{bmatrix} \theta_{p1} \\ \theta_{p2} \\ \theta_{p3} \end{bmatrix} = \begin{bmatrix} \pi/2 \\ 7\pi/6 \\ -\pi/6 \end{bmatrix} \tag{2}$$

One can then write

$$\mathbf{p}_i = \mathbf{p} + \mathbf{Q}\mathbf{r}_i' \tag{3}$$

where $\mathbf{Q}$ is the rotation matrix corresponding to the orientation of the platform of the manipulator with respect to the base coordinate frame.

The parallel mechanisms studied here comprise two main components, namely, the constraining leg, which can be thought of as a serial mechanism and the actuated legs acting in parallel.

In order to solve the inverse kinematic problem, one must first consider the passive constraining leg as a serial 3-dof mechanisms whose 3 Cartesian coordinates are known, which is a well known problem. Once the solution to the inverse kinematics of this 3-dof serial mechanism is found, the complete pose (position and orientation) of the platform can be determined using the direct kinematic equations for this serial mechanism.

For the actuated parts, subtracting vector $\mathbf{b}_i$ from both sides of eq. (3), one obtains

$$\mathbf{p}_i - \mathbf{b}_i = \mathbf{p} + \mathbf{Q}\mathbf{r}_i' - \mathbf{b}_i, \quad i = 1, 2, 3 \tag{4}$$

Then, taking the Euclidean norm of both sides of eq. (4), one derives

$$\|\mathbf{p}_i - \mathbf{b}_i\| = \|\mathbf{p} + \mathbf{Q}\mathbf{r}_i' - \mathbf{b}_i\| = \rho_i, \quad i = 1, 2, 3 \tag{5}$$

where ρ_i is the length of the ith leg, i.e. the value of the ith joint coordinate. The solution of the inverse kinematic problem for the two mechanisms is therefore completed and can finally be written as

$$\rho_i^2 = (\mathbf{p}_i - \mathbf{b}_i)^T(\mathbf{p}_i - \mathbf{b}_i), \quad i = 1, 2, 3 \tag{6}$$

4. KINEMATIC MODELING FOR THE PASSIVE LEG

The parallel mechanism studied here comprises two main components, namely, the constraining leg, which can be thought of as a serial mechanism and the actuated legs acting in parallel.

4.1. Case with rigid links

4.1.1. The Tricept machine tools. Figure 5 illustrates the configuration of the passive leg of the Tricept machine tool, From the Figure 5, we can obtain the Denavit-Hartenberg parameters as in Table I. With the Denavit-Hartenberg

Table I. The DH parameters for the pasive leg of the Tricept machine tool.

i	a_i	b_i	α_i	θ_i
0	0	0	90	0
1	0	0	90	θ_{41}
2	0	0	90	θ_{42}
3	0	Z	0	90

https://doi.org/10.1017/S0263574704000992 Published online by Cambridge University Press

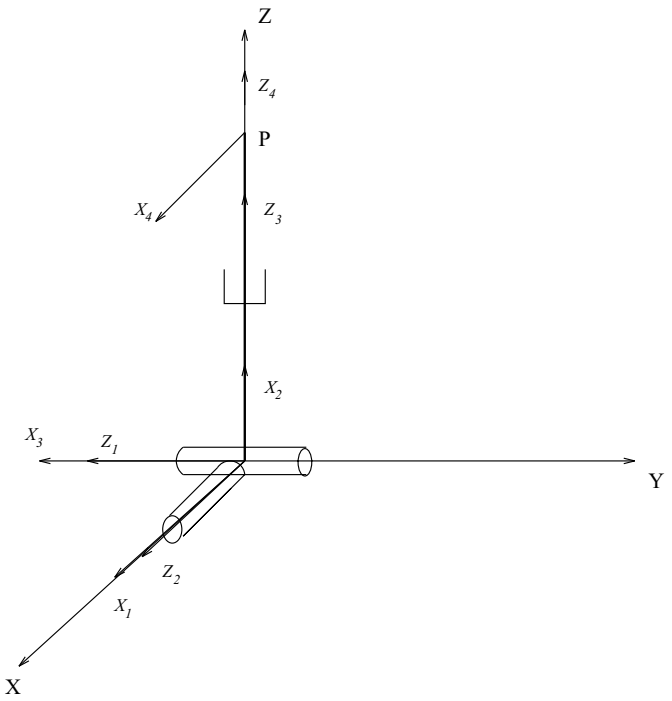

Fig. 5. The passive leg of the Tricept (rigid case).

parameters above, one can obtain the kinematic model in next section. For the passive kinematic chain, one has the velocity equation

$$\mathbf{J}_4\dot{\boldsymbol{\theta}}_4 = \mathbf{t} \tag{7}$$

where

$$\dot{\boldsymbol{\theta}}_4 = [\dot{\theta}_{41} \quad \dot{\theta}_{42} \quad \dot{\rho}]^T \tag{8}$$

and where $\mathbf{t}$ is the twist of the platform, written as $\mathbf{t} = \left[\boldsymbol{\omega}^T \ \dot{\mathbf{p}}^{\mathbf{T}}\right]^T$, where $\boldsymbol{\omega}$ the angular velocity of the platform, and the Jacobian matrix of the passive leg of the Tricept, $\mathbf{J}_4$ can be expressed as

$$\mathbf{J}_4 = \begin{bmatrix} \mathbf{e}_{41} & \mathbf{e}_{42} & \mathbf{0} \\ \mathbf{e}_{41} \times \mathbf{r}_{41} & \mathbf{e}_{42} \times \mathbf{r}_{42} & \mathbf{e}_{41} \end{bmatrix} \tag{9}$$

where $\mathbf{e}_{4i}$ is a unit vector defined in the direction of axis i while $\mathbf{r}_{4i}$ is a vector connecting the origin of frame i to point P.

4.1.2. The modified Tricept machine tool. Figure 6 illustrates the configuration of the passive leg of the modified Tricept machine tool, from the Figure 6, we can obtain the Denavit-Hartenberg parameters as in Table II. For the passive kinematic chain, we have the same velocity equation

$$\mathbf{J}_{m4}\dot{\boldsymbol{\theta}}_{m4} = \mathbf{t} \tag{10}$$

where

$$\dot{\boldsymbol{\theta}}_{m4} = [\,\dot{\rho} \quad \dot{\theta}_{m42} \quad \dot{\theta}_{m43}\,]^T \tag{11}$$

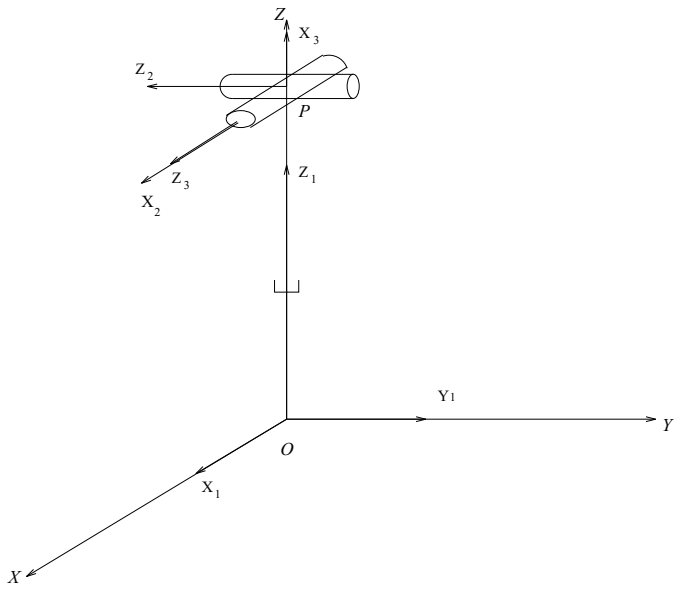

Fig. 6. The passive leg of the modified Tricept machine tool (rigid case).

Table II. The DH parameters for the passive leg of the modified Tricept machine tool.

i	a_i	b_i	α_i	θ_i
0	0	0	0	0
1	0	Z	90	0
2	0	0	90	θ_{m42}
3	0	0	0	θ_{m43}

and the Jacobian matrix of the 4th leg of the modified Tricept machine tool, $\mathbf{J}_{m4}$ can be expressed as

$$\mathbf{J}_{m4} = \begin{bmatrix} \mathbf{0} & \mathbf{e}_{42} & \mathbf{e}_{43} \\ \mathbf{e}_{41} & \mathbf{e}_{42} \times \mathbf{r}_{42} & \mathbf{e}_{43} \times \mathbf{r}_{43} \end{bmatrix} \tag{12}$$

4.2. Case with flexible links

In order to obtain a simple kinetostatic model, link compliances are lumped at the joints as described in reference [15]. In this framework, link bending stiffnesses are replaced by equivalent torsional springs located at virtual joints, as described in reference [19]. Actuator stiffnesses are also included and modeled as torsional or linear springs for revolute and prismatic actuators, respectively.

4.2.1. Tricept machine tools. Figure 7 illustrates the configuration of the passive leg with the consideration of link flexibility. Since there are forces and moments acting on the platform, the induced deformations are modeled using a virtual revolute joint on the base and two orthogonal virtual revolute joints in the middle of the passive constraining leg. These joints are drawn using dashed lines in Figure 7.

The Denavit-Hartenberg parameters can be obtained in Table III.

The kinematic chain can be taken as a serial manipulator, the kinematics of the serial manipulators comprises the study of the relations between joint variables and Cartesian

https://doi.org/10.1017/S0263574704000992 Published online by Cambridge University Press

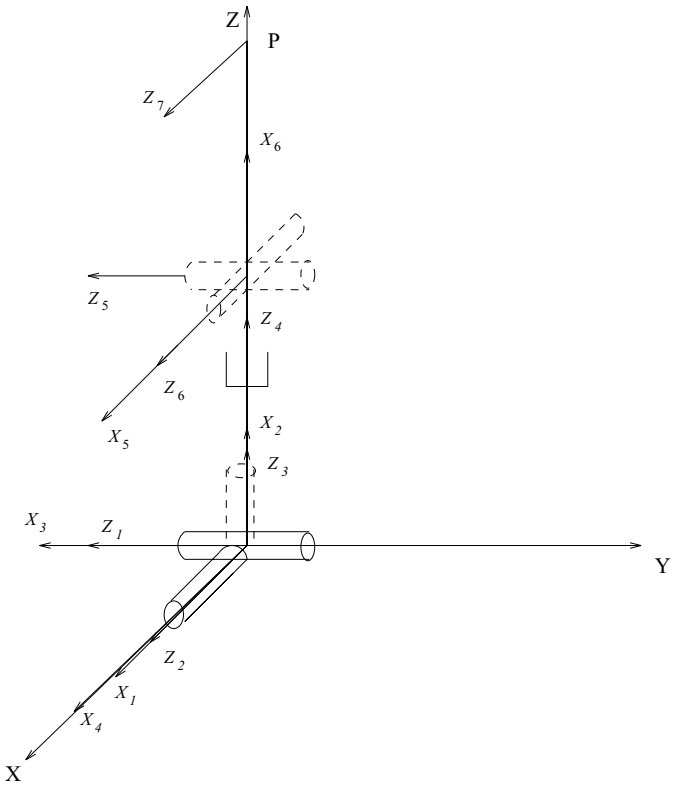

Fig. 7. The passive leg of the Tricept machine tools (with flexible links).

Table III. The DH parameters for the passive leg of the Tricept machine tool with flexible links.

i	a_i	b_i	α_i	θ_i
0	0	0	90	0
1	0	0	90	θ_{41}
2	0	0	90	θ_{42}
3	0	0	0	θ_{43}
4	0	$z/2$	90	θ_{44}
5	0	0	90	θ_{45}
6	$z/2$	0	0	θ_{46}

variables. A U-joint can be replaced by two orthogonal revolute joints in our this case.

For the passive kinematic chain, we have the velocity equation by using the same method as in the section of rigid links.

$$\mathbf{J}_4'\dot{\boldsymbol{\theta}}_4' = \mathbf{t} \tag{13}$$

where

$$\dot{\boldsymbol{\theta}}_4' = [\dot{\theta}_{41} \quad \dot{\theta}_{42} \quad \dot{\theta}_{43} \quad \dot{z}/2 \quad \dot{\theta}_{45} \quad \dot{\theta}_{46}]^T \tag{14}$$

and the Jacobian matrix of the passive leg of the Tricept, $\mathbf{J}_4$ can be expressed as

$$\mathbf{J}_4' = \begin{bmatrix} \mathbf{e}_{41} & \dots & 0 & \mathbf{e}_{45} & \mathbf{e}_{46} \\ \mathbf{e}_{41} \times \mathbf{r}_{41} & \dots & \mathbf{e}_{44} & \mathbf{e}_{45} \times \mathbf{r}_{45} & \mathbf{e}_{46} \times \mathbf{r}_{46} \end{bmatrix} \tag{15}$$

The part for the three identical legs are the same as in the rigid part.

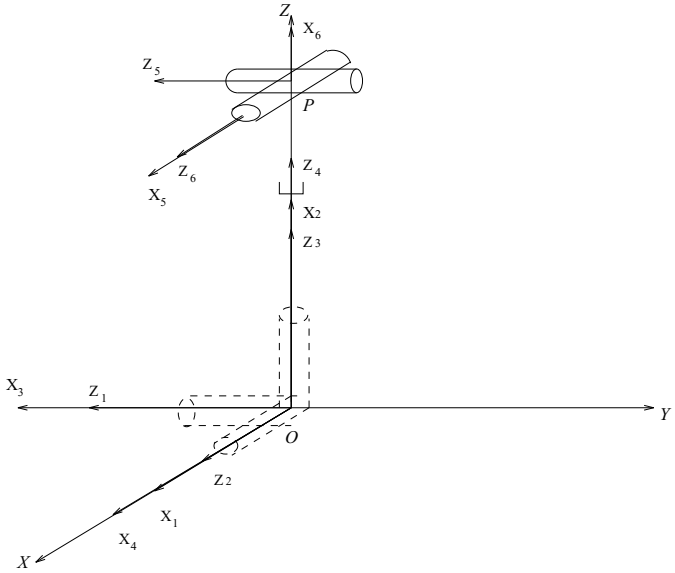

Fig. 8. The passive leg of the modified Tricept machine tool with flexible links.

Table IV. The DH parameters for the passive leg of the modified Tricept machine tool with flexible links.

i	a_i	b_i	α_i	θ_i
0	0	0	90	0
1	0	0	90	θ_{m41}
2	0	0	90	θ_{m42}
3	0	0	0	θ_{m43}
4	0	b4	90	θ_{m44}
5	0	0	90	θ_{m45}
6	0	0	0	θ_{m46}

4.2.2. The modified Tricept machine tool. Figure 8 illustrates the configuration of the passive leg of the modified Tricept machine tool with flexible links.

From Figure 8, we can obtain the Denavit-Hartenberg parameters as in Table IV. For the passive kinematic chain, we have the velocity equation by using the same method as in section of rigid links.

$$\mathbf{J}_{m4}'\dot{\boldsymbol{\theta}}_{m4}' = \mathbf{t} \tag{16}$$

where

$$\dot{\boldsymbol{\theta}}_{m4}' = [\dot{\theta}_{m41} \quad \dot{\theta}_{m42} \quad \dot{\theta}_{m43} \quad \dot{\rho}_{m44} \quad \dot{\theta}_{m45} \quad \dot{\theta}_{m46}]^T \tag{17}$$

and the Jacobian matrix of the passive leg of the mechanism $\mathbf{J}_4$ can be expressed as

$$\mathbf{J}_{m4}' = \begin{bmatrix} \mathbf{e}_{41} & \dots & 0 & \mathbf{e}_{45} & \mathbf{e}_{46} \\ \mathbf{e}_{41} \times \mathbf{r}_{41} & \dots & \mathbf{e}_{44} & \mathbf{e}_{45} \times \mathbf{r}_{45} & \mathbf{e}_{46} \times \mathbf{r}_{46} \end{bmatrix} \tag{18}$$

5. GLOBAL VELOCITY EQUATION

Now considering the parallel component of the mechanism, the parallel Jacobian matrix can be obtained by differentiating eq. (6) with respect to time, one obtains

$$\rho_i\dot{\rho}_i = (\mathbf{p}_i - \mathbf{b}_i)^T\dot{\mathbf{p}}_i, \quad i = 1, 2, 3 \tag{19}$$

https://doi.org/10.1017/S0263574704000992 Published online by Cambridge University Press

Hence one has the velocity equation as

$$\mathbf{A}\mathbf{t} = \mathbf{B}\dot{\boldsymbol{\rho}} \tag{20}$$

where vectors $\dot{\boldsymbol{\rho}}$ and $\mathbf{t}$ are defined as

$$\dot{\boldsymbol{\rho}} = [\dot{\rho}_1 \quad \dot{\rho}_2 \quad \dot{\rho}_3]^T \tag{21}$$

$$\mathbf{t} = [\omega_1 \quad \omega_2 \quad \omega_3 \quad \dot{x} \quad \dot{y} \quad \dot{z}]^T \tag{22}$$

$\omega_1, \omega_2, \omega_3$ are the angular velocities of the platform, and

$$\mathbf{A} = \begin{bmatrix} \mathbf{a}_1^T \\ \mathbf{a}_2^T \\ \vdots \\ \mathbf{a}_6^T \end{bmatrix} \tag{23}$$

$$\mathbf{B} = diag[\rho_1, \rho_2, \rho_3] \tag{24}$$

where $\mathbf{a}_i$ is a six dimension vector, which can be expressed as

$$\mathbf{a}_i = \begin{bmatrix} (\mathbf{Q}\mathbf{r}_i') \times (\mathbf{p}_i - \mathbf{b}_i) \\ (\mathbf{p}_i - \mathbf{b}_i) \end{bmatrix} \tag{25}$$

Hence, eq. (10) or (16) relates the twist of the platform to the joint velocities of the passive leg through the serial Jacobian matrix $\mathbf{J}_4$ or $\mathbf{J}_4'$ while eq. (20) relates the twist of the platform to the actuator velocities through parallel Jacobian matrices $\mathbf{A}$ and $\mathbf{B}$. It should be pointed out that the dimensions of matrix $\mathbf{J}_4$ will be (6×3), matrix $\mathbf{J}_4'$ will be (6×6), matrix $\mathbf{A}$ will be (3×6) and matrix $\mathbf{B}$ will be (3×3). The derivation of the relationship between Cartesian velocities and joint rates is thereby completed.

6. KINETOSTATIC MODELS

6.1. Case with rigid links

In this section, the velocity equations derived in the previous section will be used to obtain the kinetostatic model for the mechanism with rigid links.

According the principle of virtual work, one has

$$\boldsymbol{\tau}^T \dot{\boldsymbol{\rho}} = \mathbf{w}^T \mathbf{t} \tag{26}$$

where $\boldsymbol{\tau}$ is the vector of actuator forces applied at each actuated joint and $\mathbf{w}$ is the wrench (torque and force) applied to the platform and where it is assumed that no gravitational forces act on any of the intermediate links.

One has $\mathbf{w} = \begin{bmatrix} \mathbf{n}^T & \mathbf{f}^T \end{bmatrix}^T$ where $\mathbf{n}$ and $\mathbf{f}$ are respectively the external torque and force applied to the platform.

Rearranging eq. (20) and substituting it in eq. (26), one obtains

$$\boldsymbol{\tau}^T \mathbf{B}^{-1} \mathbf{A}\mathbf{t} = \mathbf{w}^T \mathbf{t} \tag{27}$$

Now, substituting eq. (10) into eq. (27), one has

$$\boldsymbol{\tau}^T \mathbf{B}^{-1} \mathbf{A}\mathbf{J}_4 \dot{\boldsymbol{\theta}}_4 = \mathbf{w}^T \mathbf{J}_4 \dot{\boldsymbol{\theta}}_4 \tag{28}$$

The latter equation must be satisfied for arbitrary values of $\dot{\boldsymbol{\theta}}_4$ and hence one can write

$$(\mathbf{A}\mathbf{J}_4)^T \mathbf{B}^{-T} \boldsymbol{\tau} = \mathbf{J}_4{}^T \mathbf{w} \tag{29}$$

The latter equation relates the actuator forces to the Cartesian wrench, $\mathbf{w}$, applied at the end-effector in static mode. Since all links are assumed rigid, the compliance of the mechanism will be induced solely by the compliance of the actuators. An actuator compliance matrix $\mathbf{C}$ is therefore defined as

$$\mathbf{C}\boldsymbol{\tau} = \Delta\boldsymbol{\rho} \tag{30}$$

where $\boldsymbol{\tau}$ is the vector of actuated joint forces and $\Delta\boldsymbol{\rho}$ is the induced joint displacement. Matrix $\mathbf{C}$ is a (3×3) diagonal matrix whose ith diagonal entry is the compliance of the ith actuator.

Now, eq. (29) can be rewritten as

$$\boldsymbol{\tau} = \mathbf{B}^T (\mathbf{A}\mathbf{J}_4)^{-T} \mathbf{J}_4{}^T \mathbf{w} \tag{31}$$

The substitution of eq. (31) into eq. (30) then leads to

$$\Delta\boldsymbol{\rho} = \mathbf{C}\mathbf{B}^T (\mathbf{A}\mathbf{J}_4)^{-T} \mathbf{J}_4{}^T \mathbf{w} \tag{32}$$

Moreover, for a small displacement vector $\Delta\boldsymbol{\rho}$, eq. (20) can be written as

$$\Delta\boldsymbol{\rho} \simeq \mathbf{B}^{-1} \mathbf{A} \Delta\mathbf{c} \tag{33}$$

where $\Delta\mathbf{c}$ is a vector of small Cartesian displacement and rotation defined as

$$\Delta\mathbf{c} = [\Delta\boldsymbol{\rho}^T \quad \Delta\boldsymbol{\alpha}^T]^T \tag{34}$$

in which $\Delta\boldsymbol{\alpha}$, the change of orientation, is defined as

$$\Delta\boldsymbol{\alpha} = vect(\Delta\mathbf{Q}\mathbf{Q}^T) \tag{35}$$

where $\Delta\mathbf{Q}$ is the variation of the orientation and $vect(\cdot)$ is the vector linear invariant of its matrix argument.

Similarly, eq. (10) can also be written, for small displacements, as

$$\mathbf{J}_4 \Delta\boldsymbol{\theta}_4 \simeq \Delta\mathbf{c} \tag{36}$$

where $\Delta\boldsymbol{\theta}_4$ is a vector of small variations of the joint coordinates of the constraining leg.

Substituting eq. (33) into eq. (32), one obtains

$$\mathbf{B}^{-1} \mathbf{A} \Delta\mathbf{c} = \mathbf{C}\mathbf{B}^T (\mathbf{A}\mathbf{J}_4)^{-T} \mathbf{J}_4^T \mathbf{w} \tag{37}$$

Premultiplying both sides of eq. (37) by $\mathbf{B}$, and substituting eq. (36) into eq. (37), one obtains,

$$\mathbf{A}\mathbf{J}_4 \Delta\boldsymbol{\theta}_4 = \mathbf{B}\mathbf{C}\mathbf{B}^T (\mathbf{A}\mathbf{J}_4)^{-T} \mathbf{J}_4^T \mathbf{w} \tag{38}$$

Then, premultiplying both sides of eq. (38) by $(\mathbf{A}\mathbf{J}_4)^{-1}$, one obtains,

$$\Delta\boldsymbol{\theta}_4 = (\mathbf{A}\mathbf{J}_4)^{-1} \mathbf{B}\mathbf{C}\mathbf{B}^T (\mathbf{A}\mathbf{J}_4)^{-T} \mathbf{J}_4^T \mathbf{w} \tag{39}$$

and finally premultiplying both sides of eq. (39) by $\mathbf{J}_4$, one obtains,

$$\Delta\mathbf{c} = \mathbf{J}_4 (\mathbf{A}\mathbf{J}_4)^{-1} \mathbf{B}\mathbf{C}\mathbf{B}^T (\mathbf{A}\mathbf{J}_4)^{-T} \mathbf{J}_4^T \mathbf{w} \tag{40}$$

Hence, one obtains the Cartesian compliance matrix as

$$\mathbf{C}_c = \mathbf{J}_4 (\mathbf{A}\mathbf{J}_4)^{-1} \mathbf{B}\mathbf{C}\mathbf{B}^T (\mathbf{A}\mathbf{J}_4)^{-T} \mathbf{J}_4^T \tag{41}$$

with

$$\Delta\mathbf{c} = \mathbf{C}_c \mathbf{w} \tag{42}$$

where $\mathbf{C}_c$ is a symmetric positive semi-definite (6×6) matrix, as expected.

https://doi.org/10.1017/S0263574704000992 Published online by Cambridge University Press

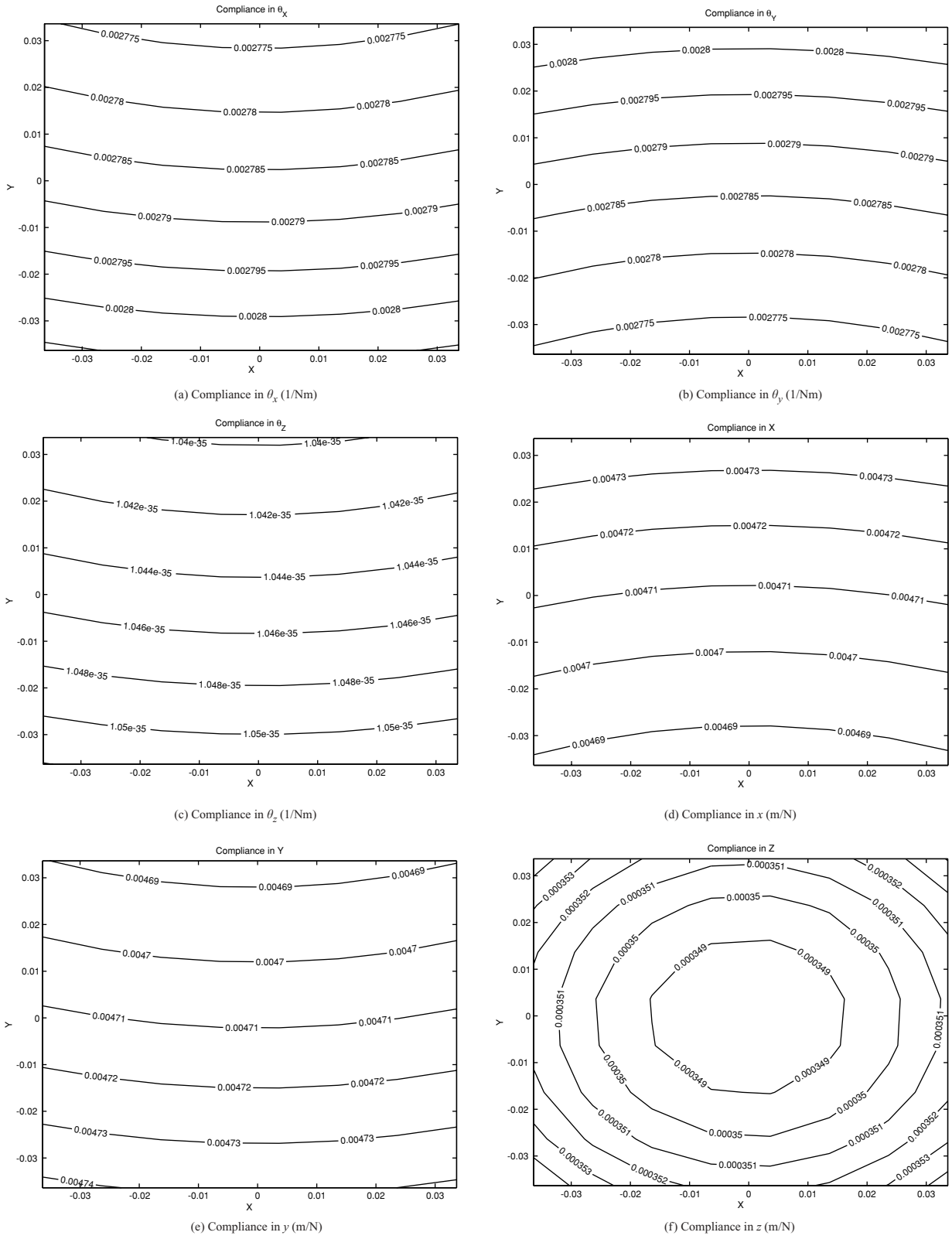

(a) Compliance in θ_x (1/Nm)

(b) Compliance in θ_y (1/Nm)

(c) Compliance in θ_z (1/Nm)

(d) Compliance in x (m/N)

(e) Compliance in y (m/N)

(f) Compliance in z (m/N)

Fig. 9. Compliance mappings of the Tricept machine tool (all length units in m).

It is pointed out that, in nonsingular configurations, the rank of $\mathbf{B}$, $\mathbf{C}$ and $\mathbf{J}_4$ is 3 and hence the rank of $\mathbf{C}_c$ will be 3. Hence, the nullspace of matrix $\mathbf{C}_c$ will not be empty and there will exist a set of vectors $\mathbf{w}$ that will induce no Cartesian displacement $\Delta\mathbf{c}$. This corresponds to the wrenches that are supported by the constraining leg, which is considered infinitely rigid. These wrenches are orthogonal complements of the allowable twists at the platform. Hence, matrix $\mathbf{C}_c$ cannot be inverted and this is why it was more convenient to use compliance matrices other than stiffness matrices in the above derivation. In the modified case, $\mathbf{J}_4$ is replaced by $\mathbf{J}_{m4}$.

In the next section, the kinetostatic model will be rederived for the case in which the flexibility of the links is considered. In this case, stiffness matrices will be used.

https://doi.org/10.1017/S0263574704000992 Published online by Cambridge University Press

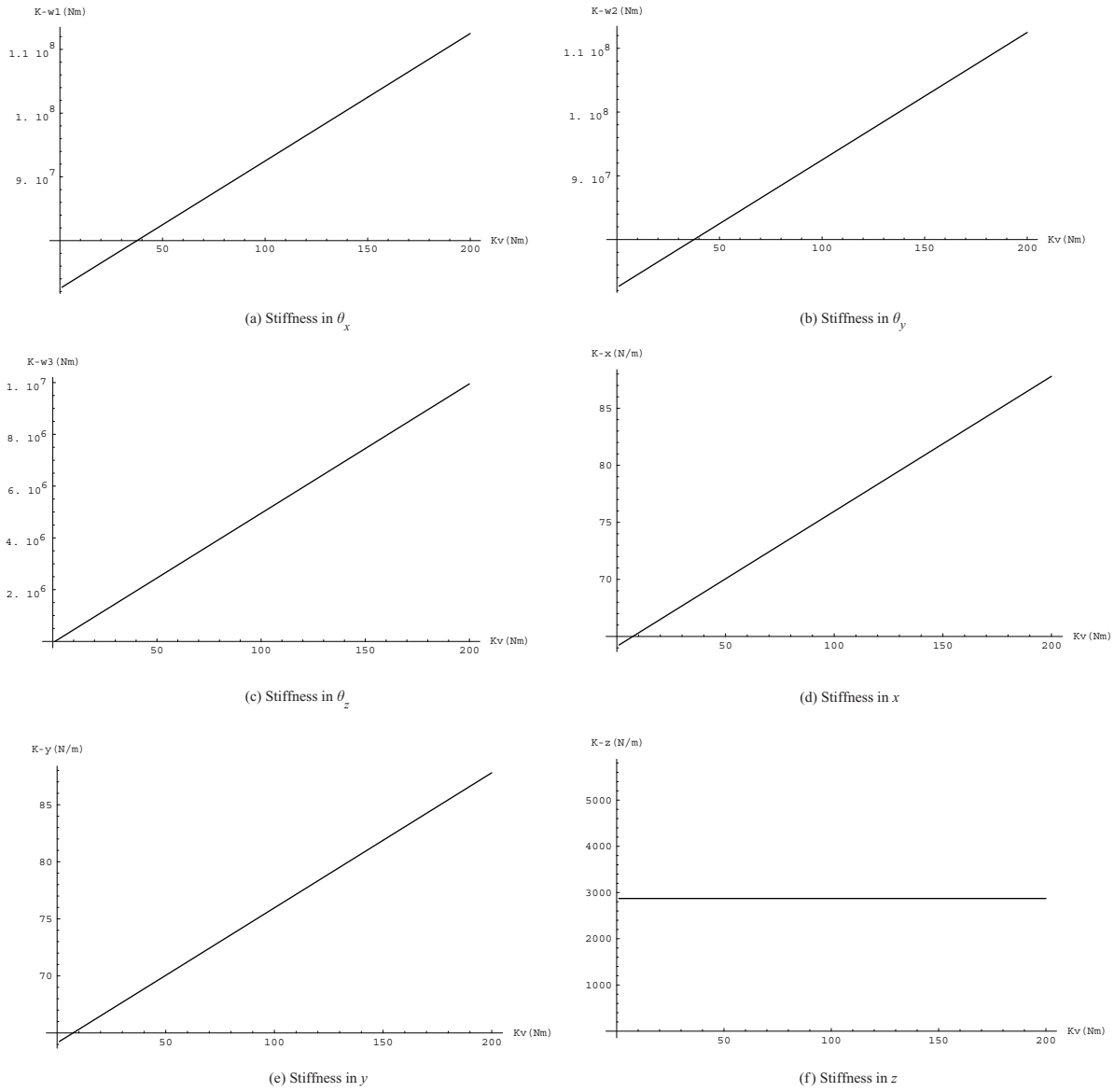

(a) Stiffness in θ_x

(b) Stiffness in θ_y

(c) Stiffness in θ_z

(d) Stiffness in x

(e) Stiffness in y

(f) Stiffness in z

Fig. 10. Evolution of the stiffness as a function of the passive link's lumped stiffness in different directions (Tricept).

6.2. *Case with flexible links*

According to the principle of virtual work, one can write

$$\mathbf{w}^T\mathbf{t} = \boldsymbol{\tau}_4^T\dot{\boldsymbol{\theta}}_4' + \boldsymbol{\tau}^T\dot{\boldsymbol{\rho}} \tag{43}$$

where $\boldsymbol{\tau}$ is the vector of actuator forces and $\dot{\boldsymbol{\rho}}$ is the vector of actuator velocities (actuated legs), and $\boldsymbol{\tau}_4$ is the vector of joint torques in the constraining leg. This vector is defined as follows, where $\mathbf{K}_4$ is the stiffness matrix of the passive leg,

$$\boldsymbol{\tau}_4 = \mathbf{K}_4\Delta\boldsymbol{\theta}_4' \tag{44}$$

$$\mathbf{K}_4(\textit{modified Tricept}) = diag[k_{41}, k_{42}, k_{43}, 0, 0, 0] \tag{45}$$

$$\mathbf{K}_4(\textit{Tricept}) = diag[0, 0, k_{43}, 0, k_{45}, k_{46}] \tag{46}$$

Matrix $\mathbf{K}_4$ is a diagonal (6×6) matrix in which the ith diagonal entry is zero if it is associated with a real joint is equal to k_i if it is associated with a virtual joint, where k_i is the stiffness of the virtual virtual spring located at the ith joint.

Eq. (43) can be rewritten as

$$\mathbf{w}^T\mathbf{t} = \boldsymbol{\tau}_4^T(\mathbf{J}_4')^{-1}\mathbf{t} + \boldsymbol{\tau}^T\mathbf{B}^{-1}\mathbf{A}\mathbf{t} \tag{47}$$

Since this equation is valid for any value of $\mathbf{t}$, we can write

$$\mathbf{w} = (\mathbf{J}_4')^{-T}\boldsymbol{\tau}_4 + \mathbf{A}^T\mathbf{B}^{-T}\boldsymbol{\tau} \tag{48}$$

which can be rewritten as

$$\mathbf{w} = (\mathbf{J}_4')^{-T}\mathbf{K}_4\Delta\boldsymbol{\theta}_4 + \mathbf{A}^T\mathbf{B}^{-T}\mathbf{K}_J\Delta\boldsymbol{\rho} \tag{49}$$

where $\mathbf{K}_J$ is a 3×3 joint stiffness matrix for the actuated joints.

Using the kinematic equations, we can then write:

$$\mathbf{w} = (\mathbf{J}_4')^{-T}\mathbf{K}_4(\mathbf{J}_4')^{-1}\Delta\mathbf{c} + \mathbf{A}^T\mathbf{B}^{-T}\mathbf{K}_J\mathbf{B}^{-1}\mathbf{A}\Delta\mathbf{c} \tag{50}$$

which is in the form

$$\mathbf{w} = \mathbf{K}\Delta\mathbf{c} \tag{51}$$

where $\mathbf{K}$ is the Cartesian stiffness matrix, which is equal to

$$\mathbf{K} = (\mathbf{J}_4')^{-T}\mathbf{K}_4(\mathbf{J}_4')^{-1} + \mathbf{A}^T\mathbf{B}^{-T}\mathbf{K}_J\mathbf{B}^{-1}\mathbf{A} \tag{52}$$

https://doi.org/10.1017/S0263574704000992 Published online by Cambridge University Press

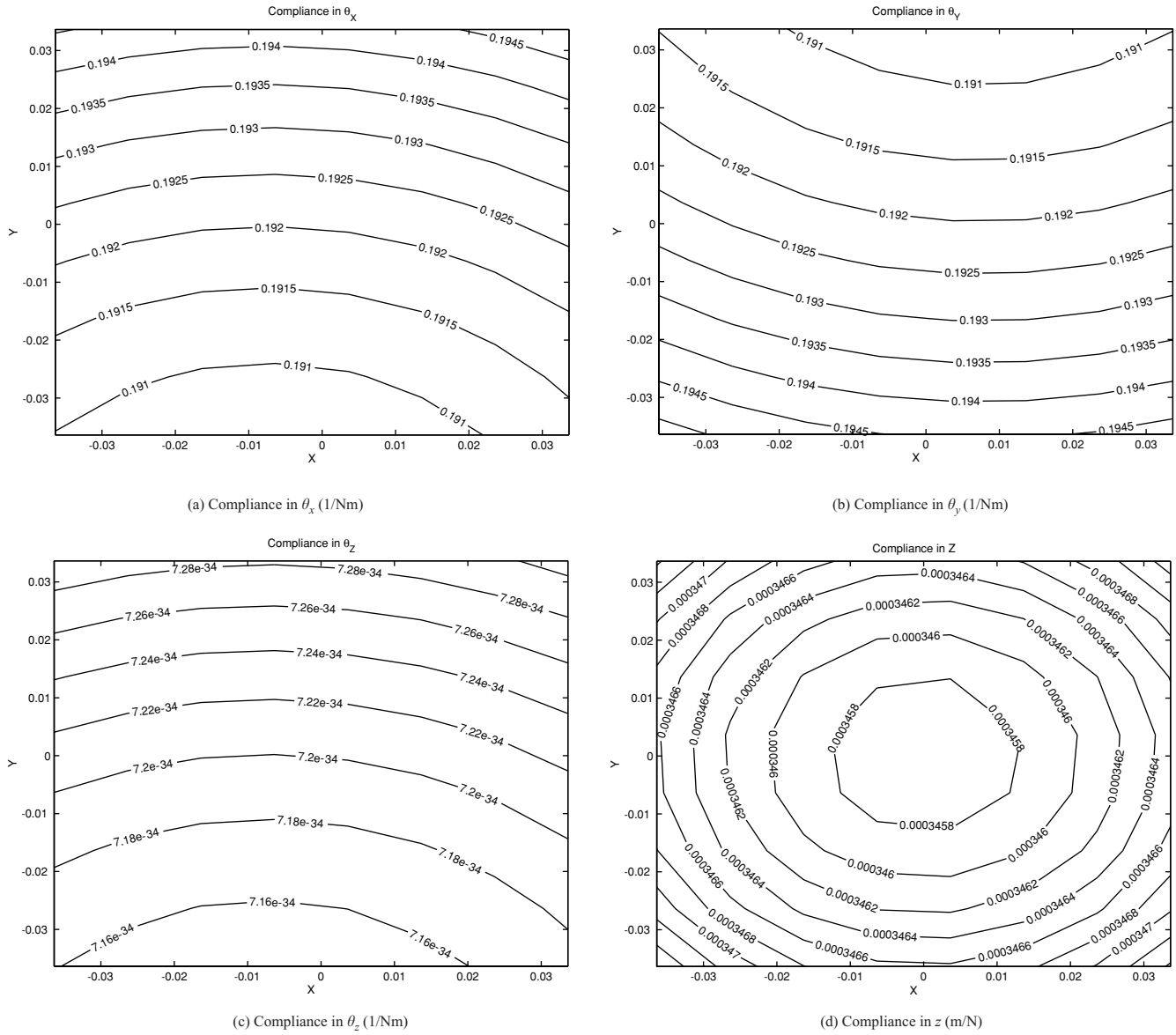

(a) Compliance in θ_x (1/Nm)

(b) Compliance in θ_y (1/Nm)

(c) Compliance in θ_z (1/Nm)

(d) Compliance in z (m/N)

Fig. 11. Compliance mappings of the Tripod-based PKM (all length units in m).

Matrix $\mathbf{K}$ is a symmetric (6×6) positive semi-definite matrix, as expected. However, in this case, matrix $\mathbf{K}$ will be of full rank in non-singular configurations. Indeed, the sum of the two terms in eq. (52) still span the complete space of constraint wrenches. In the modified case, $\mathbf{J}'_4$ is replaced by $\mathbf{J}'_{m4}$.

7. IMPLEMENTATION

The parameters used in this example are given by SMT Tricept AB as follows:

$$\theta_{b1} = \pi/2, \theta_{b2} = 7\pi/6, \theta_{b3} = -\pi/6,$$
$$\theta_{p1} = \pi/2, \theta_{p2} = 7\pi/6, \theta_{p3} = -\pi/6,$$
$$R_p = 225 \text{ mm}, R_b = 500 \text{ mm},$$
$$k_{i1} = 1000 \text{ N/m}, \quad i = 1, 2, 3$$

where k_{i1} is the actuator stiffness and the Cartesian coordinates are given as

$$x \in [-2, 2] \text{ cm}, y \in [-2, 2] \text{ cm}, z = 1300 \text{ mm},$$
$$\theta_{41} = \pi/2, \theta_{42} = \pi/2,$$

From eq. (52), the stiffness for passive leg can be written as

$$\mathbf{K} = (\mathbf{J}'_4)^{-T} \mathbf{K}_4 (\mathbf{J}'_4)^{-1} \tag{53}$$

We implemented the above model for both Tricept machine tool and modified Tricept machine tool to compare the difference of installing U-joint at the base and at the moving platform. Given the same geometric sizes and other parameters, i.e. the dimentions for moving platform and base platform, the passive leg length, diameter and material, the actuators and length for all three actuated prismatic joints. For both the Tricept machine tool and the modified Tricept machine tool, assuming the bending stiffness of the passive leg in both X and Y directions is 100000 N/m, and torsional stiffness of the passive leg is 100000 Nm. Based on the

https://doi.org/10.1017/S0263574704000992 Published online by Cambridge University Press

Table V. Comparison of the global stiffness contributed by the passive leg.

(N/m)	K_{θ_x} (Nm)	K_{θ_y} (Nm)	K_{θ_z} (Nm)	K_x (N/m)	K_y (N/m)	K_z
Tricept	4×10^5	4×10^5	1×10^5	4.93827×10^5	4.93827×10^5	0
Modified Tricept	0	0	1×10^5	1×10^6	1×10^6	0

kinetostatic models, it's easy to obtain the following results (Table V).

The results are quite reasonable, as for Tricept machine tool, the rotations in X and Y are compound ones rather than pure rotation, therefore, there still exists stiffness in θ_x and θ_y. For the modified Tricept machine tool, the rotations around X and Y are pure rotation, the torsional stiffness in these two directions are 0. It has been observed that Tripod with U-joint in the moving platform is more rigid than Tripod with U-joint installed at the base. The modified Tricept machine tool is two times stiffer than that of the Tricept machine tool.

8. STIFFNESS MAPPINGS

Since we are now discussing the manipulator with 3dof, and there should exist three infinite stiffnesses in three of the directions, hence instead of a stiffness matrix, we applied a compliance matrix. The analysis described above will now be used to obtain the compliance maps for spatial three-degree-of-freedom parallel manipulators. The maps are drawn on square areas of the variation of the end-effector's position.

Visualization tools to aid in the use of such expressions have been developed. A program has been written on Mathematica software, after giving the initial values above, then the contour maps can be shown in Figure 9, from such plots one can determine which regions of the workspace will satisfy some compliance criteria.

From Figure 10, it can be seen that K_{θ_x}, K_{θ_y}, K_{θ_z}, K_x and K_y are becoming infinite while the flexible links are becoming rigid, and K_z is kept constant, it corresponds to the motions prevented by the passive constraining leg and at this configuration, the motions along the X and the Y are also limited (for passive leg is welded with platform).

In Figures 11(a) and 11(b), the torsional compliances in θ_x and θ_y are shown, the compliances are symmetric. In Figure 11(d) the stiffness in z is higher near the center of the workspace, which is the best position for supporting vertical loads. This is due to the architecture chosen, which aims at supporting heavy objects in an environment where the gravity is acting along the negative direction of z axis. All these are in accordance with what would be intuitively expected.

9. CONCLUSIONS

In this paper, a modified Tricept machine tool with a different passive leg structure is presented. The kinetostatic models for both the original Tricept machine tool and the modified Tricept machine tool are generated. The comparison of the two configurations is conducted in terms of global stiffness and compliance mapping. It is shown that a Tricept with a U-joint installed at the moving platform is more rigid than that of a Tricept with a U-joint installed at the base platform. The influence of the different arrangement of the joint in the passive leg is analyzed and pointed out.

References

1. V. Gough, "Contribution to discussion to papers on research in automobile stability and control and in tire performance," *Proceedings of the Auto. Div. Instn mech. Engrs.* (1956) p. 392.
2. D. Stewart, "A platform with six degrees of freedom, In Proceedings of the Institution of Mechanical Engineers," **180**, 371–378 (1965).
3. S. K. Advani, *The Kinematic Design of Flight Simulator Motion-Bases* (Delft University Press, 1998).
4. C. Reinholz and D. Gokhale, "Design and analysis of variable geometry truss robot," *Proc. 9th Applied Mechanisms Conference*. U.S.A. (1987) pp. 1–5.
5. T. Arai, K. Cleary, K. Homma, H. Adachi and T. Nakamura, "Development of parallel link manipulator for underground excavation task," *1991 International Symposium on Advanced Robot Technology* (1991) pp. 541–548.
6. C. M. Gosselin and J. Hamel, "The agile eye: A high-performance three-degree-of-freedom camera-orienting device," *Proceedings of the IEEE International Conference on Robotics and Automation* (1994) pp. 781–786.
7. Physik-Instrumente, "Hexapod 6 axis micropositioning system," **In**: *Supplement to the catalog No. 111/112*, pp. 36–37 (1997).
8. J. Lauffer, T. Hinnerichs, C. P. Kuo, B. Wada, D. Ewaldz, B. Winfough and N. Shankar, "Milling machine for the 21st century – goals, approach, characterization and modeling," *Proceedings of SPIE – The International Society for Optical Engineering Smart Structures and Materials* 1996: Industrial and Commercial Applications of Smart Structures Technologies. San Diego (Feb., 1996) **Vol**. 2721, pp. 326–340.
9. P. Bailey, "The merits of hexapods for robotics applications," *Conference on next steps for industrial Robotics*, London (1994) pp. 11/8–16/8.
10. J. Hollingum, "Features: Hexapods to take over?," *Industrial Robot* **24**, 428–431 (1997).
11. M. Valenti, "Machine tools get smarter," *ASME Mechanical Engineering* **117**, 70–75 (1995).
12. J. Kim et al., "Performance analysis of parallel manipulator architectures for cnc machining," *1997 ASME IMECE Symposium on Machine Tools* (1997) pp 341–348.
13. K.-E. Neumann, *Robot* (United States Patent, Patent Number: 4,732,525, 1988).
14. B. Whitworth, "More axes to grind," *Professional Engineering* No. 2, 40–42 (1998).
15. D. Zhang, "Kinetostatic Analysis and Optimization of Parallel and Hybrid Architectures for Machine Tools," *Ph.D. thesis* (Laval University, Québec, Canada, 2000).
16. H. K. Tönshoff, H. Grendel and R. Kaak, "Structure and characteristics of the hybrid manipulator georg v," **In**: *Parallel Kinematic Machines — Theoretical Aspects and Industrial Requirements* (editors: C. R. Boër, L. Molinari-Tosatti and K. S. Smith) (Springer Publishers, 1999) pp. 365–376.
17. H. K. Tönshoff, C. Soehner and H. Ahlers, "A new machine tool concept for laser machining," *Proceedings of International Seminar on Improving Machine Tool Performance*, San Sebastin (1998) pp. 199–224.
18. J. Lewis, "Tripod-mounted spindle targets monolithic parts," *Design News* 54–58 (2000).
19. D. Zhang and C. M. Gosselin, "Kinetostatic modeling of n-dof parallel mechanisms with a passive constraining leg and prismatic actuators," *ASME Journal of Mechanical Design* **123**, No. 3, 375–381 (2001).

https://doi.org/10.1017/S0263574704000992 Published online by Cambridge University Press